Final Report
Muon Physics

Benjamin Freiman
Section 1.

(Dated: August 15, 2022)

Through the use of a scintillator, a photomultiplier and a discriminator along with an FPGA timer, the mean lifetime decay time for a muon at rest is calculated. The experiment confirmed the effects of special relativity on the decay time of muons. Through the extraction of the mean decay time for a muon $t_{decay} = 2.10\mu s \pm 0.06\mu s$, the Fermi coupling constant $G_F = 1.20 \times 10^{-5} \pm 0.2 \times 10^{-5} (GeV)^{-2}$ was validated upholding the knowledge that muons undergo beta decay via the weak force. It was determined that negatively charged muons interact with protons in the scintillator by obtaining a value of $\rho = 1.55 \pm 0.02$ for the charge ratio of positively and negatively charged muons.

I. INTRODUCTION

Every second, muons that originate from the upper atmosphere course through your body. Muons are a subatomic particle similar to an electron with a much greater mass and fast decay time. Sometimes these muons can actually decay into an electron and two neutrinos in your body. However, muons should decay in around $2.2\mu s$. Because they are traveling at a speed close to that of light, without any consideration of time dilation, the muons should decay within $0.5km$. With the muons originating from the upper atmosphere (due to high energy particles from other places in the universe), there is one caveat. The muons should not be found on earth. However, this lab report proves the detection of muons and their decay. The reasoning behind this is special relativity and time dilation. When an object travels at a speed comparable to that of the speed of light, assuming the muon is going .99 times the speed of light, the time for a muon decay from the reference frame on earth is defined by equation (1) where Δt_{earth} is the decay time from the reference frame on earth for a muons decay time and Δt_{muon} is the decay time from the reference frame of a muon. c is the speed of light and v is the velocity of the muon with respect to the earth.

$$\Delta t_{earth} = \frac{\Delta t_{muon}}{\sqrt{1 - \frac{v^2}{c^2}}} = 15.595\mu s, \tag{1}$$

Equation (1) demonstrates changes in the decay time by around a factor of 7. Because of the the linear relationship of time and distance, srather than taking .5 km to decay, the muon will now take 3.5 km to decay. Taking into account that the muon is going faster than .99c, it is made clear that the muons actually should be detected at the earth's surface under the effect of time dilation. The muon distribution of decay times in any reference frame follows an exponential decay. It is apparent that the number of muons decaying is independent of the reference frame and solely dependent on the elapsed time. This independence on the reference frame leads to the exponential distribution occurring at any reference frame where the equation 2 holds. N is the number of muons. ΔN is the change in the number of muons which is negative in all cases due to decays of muons into other subatomic particles. Δt is the change in time. λ is equal to the constant $\frac{1}{t_{decay}}$. Essentially, the change in the number of muons under a time frame is equal to a negative constant times the amount of initial muons because the number of muons will always decrease under the assumption that no new muons are added to N.

$$\frac{\Delta N}{\Delta t} = -\lambda N, \tag{2}$$

Upon taking the limit $\Delta N \to 0$ and $\Delta t \to 0$, equation (3) arises.

$$N = N_0 e^{-\lambda t}, \tag{3}$$

Assuming that the time of decay has to be greater than 0, as the lower limit of decay time t_{decay} approaches 0, the negative exponential $e^{-\frac{1}{t_{decay}}t} \to e^{-\infty}$approaches a maximum at $N = \infty$. At the upper limit of the exponential where $t_{decay} \to \infty$ the number of decays goes to zero. This displays that the muon decay distribution is a maximum for decay times close to $t_{decay} = 0$ and a minimum at $t_{decay} = \infty$ independent of the reference frame measured in. The implications of this on the experiment is the number of decays across a long period of time should show a distribution with many muons near decay times of $t_{decay} = 0$ and fewer muons near $t = 40\mu s$ following this negative exponential decay. Clearly there is no dependence on reference frame, and this allows the effective measurement of the muon decay time on Earth's surface without being within the muons reference frame. The calculation of mean decay time or t_{decay} is made by fitting the exponential decay function in Python, using the scipy.odr library, to the muon decay distribution as a histogram with bin sizes of $0.5\mu s$, $1\mu s$ and $2\mu s$ and extracting the parameter lambda results in the easy calculation of t_{decay} through the relation $\lambda = \frac{1}{t_{decay}}$. Once the best fit for muon decay time is discovered and the mean decay time t_{decay} is extracted, an accurate approximation of the Fermi coupling constant is made. The

Fermi coupling constant is a constant directly related to the weak force. The weak force can be thought of as the force that breaks symmetry in space and time, causing decays in subatomic particles like muons. In physics the implication of this is beta decay. In this experiment the Fermi coupling constant is derived and proves the muons undergo beta decay through the weak force. In addition, the charge ratio from positive to negative muons is calculated. A charge ratio greater than one indicates that there are more decays of positive muons than negative muons. This phenomenon arises due to how the negative muons interact with protons in the scintillator. It is expected that some of the negatively charged muons fill a proton's orbital resulting in a charge ratio slightly greater than one. The goals of this experiment are to calculate the mean lifetime decay of muons at rest, along with the Fermi coupling constant and the charge ratio of positive to negative muons.

II. EXPERIMENTAL METHODS

The experimental apparatus was set up in a way where the muons rain down from the sky and into the scintillator. In figure (1) the muon is seen entering the scintillator and decaying into an electron and two neutrinos. The material within this device contains flora that emit light when struck by the muon but also any other charged or high energy particle. There is a great importance of filtering out decays of muons and the detection of other particles. Once the signal is filtered by the discriminator, the

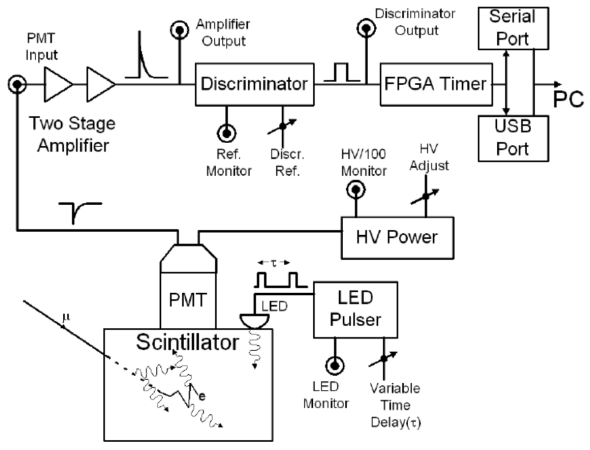

FIG. 1. The circuitry and the apparatus used to send decay times to the computer.

FPGA timer times the first pulse from when the muon enters the apparatus to the second pulse of the decay. If the elapsed time between pulses is not within $\Delta t > 40\mu s$ then the signal is not considered and the timing circuit is restarted. The signal is not considered because of the likelihood of this not being a muon. The first task was to ensure that the instruments were calibrated and there were not any issues. Testing that the gain was correctly measured for different frequencies meant that, no matter the frequency of the wave, the voltage input and output signal would not be distorted. As seen in figure (2) the implication of this is when the frequency gets too large or too small the frequency vs gain becomes linear.

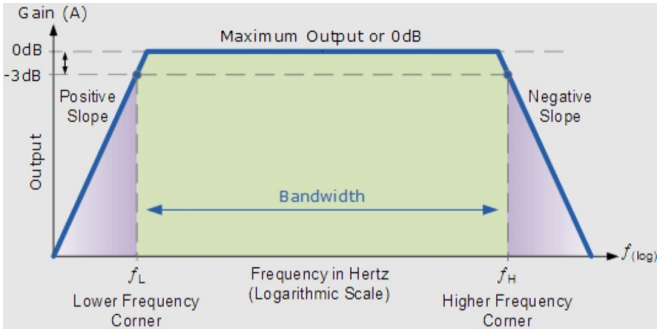

FIG. 2. Frequency V.S. Gain Distortion.

Despite using all of the frequencies possible in our function generator, this never happened and the gain was constant and the frequency was within the middle part of the trapezoid where gain is constant. Next, it was ensured that discriminator voltage goes up as time difference goes down. This means that the voltage output will be really small when the time difference is large. It also implies that the voltage must be transmitted at lower times where muon decays are more frequent.

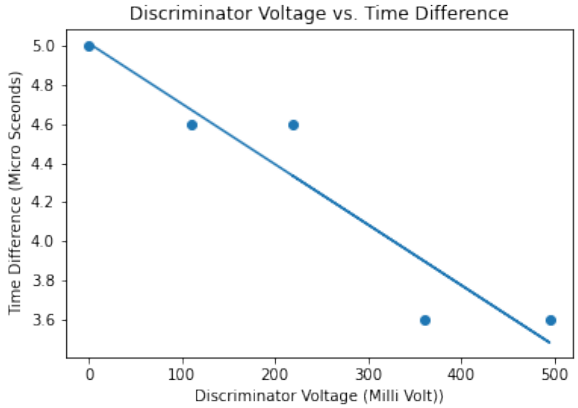

FIG. 3. As the time between decays or pulses goes down, the voltage transmitted goes up due to the likelihood of it being a muon decay.

By finding a good discriminator voltage, the circuit only transmitted voltages that were caused by muons. The implications for this experiment were that background radiation causing higher voltages were not transmitted and did not appear in the data. Finally, the calibration of the software detecting the timings between pulses was recorded. By measuring the rising edges from the oscilloscope, and then looking at the timings on the muon

Bin Size (μs)	Bin Error (%)	Decay Time (μs)	Error (μs)	β (decays)	Error (decays)	$\tilde{\chi}^2$
.5	10	2.10	0.04	1.2	0.4	0.546
.5	20	2.11	0.04	1.2	0.4	0.523
.5	30	2.11	0.05	1.1	0.4	0.497
1	10	2.10	0.06	3.0	0.8	1.04
1	20	2.11	0.07	3.0	0.8	0.957
1	30	2.11	0.09	3.0	0.7	0.892
2	10	2.11	0.05	8	2	0.209
2	20	2.12	0.07	8	2	0.173
2	30	2.11	0.09	8	2	0.140

TABLE I. List of muon decay fits.

software, it would be made clear after running the software for 30 seconds, how accurate each imitation decay time was. This was done by measuring the difference in time between the rising edge time on the oscilloscope and comparing that time to that of the software averages. After running the software for 30 minutes was clear that there was a negative exponential decay in the distribution of muon decays, and mose decays were under $t = 10\mu s$, and less decays at $t = 20\mu s$. Upon proper calibration of the circuit and data collection for forty eight hours, the data was ready to be analyzed.

III. ANALYSIS AND RESULTS

The data was fit to a negative exponential of the form $f(t) = Ne^{-\frac{1}{t_{decay}}t} + \beta$ where t_{decay} is a constant. The β term is introduced in case background radiation or noise of any kind can be accounted for by a vertical shift. In table (1) it is clear that the β term is proportional to the bin width and is systematic.

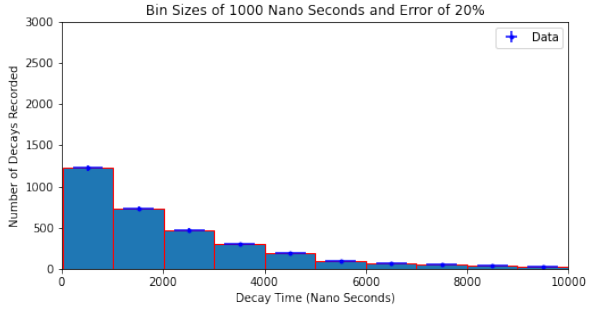

FIG. 4. Histogram of Muon Decays as a Function of Decay Time.

This vertical shift and background noise was essential in getting an accurate fit. After fitting an exponential decay function to the nine permutations of bin width sizes equal to $0.5\mu s$ $1\mu s$ and $2\mu s$ with bin width error equal to %10, %20 and %30 the results in Table 1 for the mean lifetime decay in a muon was also obtained. The histograms that were later fit to an exponential are similar to figure (4). The fits used the square root of the y value for the y-error.

Considering all nine permutations of bin size and bin error, the reduced chi-squared value of $\tilde{\chi}^2 = 1.04$ is closest to $\tilde{\chi}^2 = 1$. Therefore the corresponding value for mean decay time $t_{decay} = 2.10\mu s \pm 0.06\mu s$ is used for the rest of the experiment. In comparison to the literature value of 2.1969811 ± 0.0000022 seconds [1], the value reported in this experiment agrees nicely. The most proper fit had a clear exponential decay with the exponential running through most of the points.

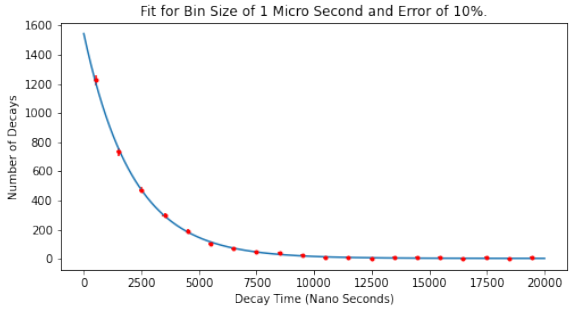

FIG. 5. Example plot.

Using the decay time the Fermi coupling constant was derived.

$$G_F = \sqrt{\frac{192\pi^3\hbar}{\tau m^5 c^4}}(Jm^3), \tag{4}$$

$$\frac{G_F}{(\hbar c)^3} = \sqrt{\frac{\hbar}{\tau_\mu} \cdot \frac{192\pi^3}{(m_\mu c^2)^5}} GeV \cdot s, \tag{5}$$

The muon decay time declared above is $\tau_\mu = 2.10 \pm .06\mu s$. Substituting $\hbar \approx 6.5821193 \cdot 10^{-25} \pm 0.0000002 \cdot 10^{-25} GeV \cdot s$ and the mass of a muon $m_\mu = 0.100 \pm .005 \frac{GeV}{c^2}$ [2] into equation (5), the relation in equation (6) is obtained.

$$G_F \tag{6}$$
$$= \sqrt{(6.5821193 \pm 0.0000002) \cdot 10^{-25} \frac{1}{.00000210 \pm .00000006}} \cdot \sqrt{\frac{192\pi^3}{(0.100 \pm .005)^5}},$$

$$G_F = 1.20 \cdot 10^{-5} \pm 0.06 \cdot 10^{-5} (GeV)^{-2}, \quad (7)$$

The Resulting value of $G_F = 1.20 \times 10^{-5} \pm 0.06 \times 10^{-5}(GeV)^{-2}$ agrees with the literature value of $G_F = 1.166378 \times 10^{-5} \pm 0.000006 \times 10^{-5}(GeV)^{-2}$ [3].

This ratio of the negative to positive is given by the equation below.

$$\rho = -\frac{\tau^-}{\tau^+}\left(\frac{\tau^- - \tau_{exp}}{\tau^+ - \tau_{exp}}\right), \quad (8)$$

Using $\tau^- = 2.043\mu s$ from the RPI Muon Physics Manual and also $\tau^+ = 2.200\mu s$ the free space lifetime value $\tau_{exp} = 2.10 \pm .06\mu s$. The result derived below was that $\rho = 1.55 \pm 0.02$.

$$\rho = -\frac{\tau^-}{\tau^+}\left(\frac{-0.06 \pm 0.06}{0.10 \pm 0.06}\right)$$
$$\rho = -\frac{2.043 \pm 0.003}{2.19703 \pm .00004}(-0.6 \pm 0.7)$$
$$\rho = -(.930 \pm 0.001)(-0.6 \pm 0.7) = 1.55 \pm 0.02$$

This value of ρ agrees closely with the charge ratios in the literature and figure (7).

IV. DISCUSSION

The thought that comes to mind in an experiment involving decay times is background noise when a subatomic particle like an electron through coulomb forces or some other force. This force causes fluorescens when the electron inside the scintillator is moved from a stable state to an excited state causing emmision of light. Noise similar to this is likely going to cause some perturbation away from the expected fit. The issue of backround noise made it difficult to interpolate (draw a curve) between the points in figure (5) and figure (6). To account for this background radiation that might not have been filtered out by the discriminator and the FPGA timer, the error range in the y-direction needed to be adjusted slightly from the square root of the y data. Upon completion nine plots were fitted with reduced chi-squared values ranging from $\tilde{\chi}^2 = 0.140 - 1.04$. The reduced chi-square value of one means that approximately two thirds of the data points are within one standard deviation. An over fit data set in figure (6) has the reduced chi-squared value of $\tilde{\chi}^2 = 0.140$. The error bars extend far to the left and right, where too many points fall within one standard deviation of the data set.

In "Charge Ratio of High-Energy Cosmic Ray Muons"[4], Hayman et al. discovers charge ratios across different momentums of muons. When comparing the charge ratios to this experiment, there is a better understanding of the mean momentum of the muons collected in this experiment at ground level. According to the table, ρ agrees with the charge ratio averaged over muons with a momentum of $120 - 240\frac{GeV}{c}$.

It is interesting to note that all of the values in the table are greater than one. This reinforces how in this experiment the charge ratio is greater than one even across different momentums due to the negatively charged muons interacting with protons.

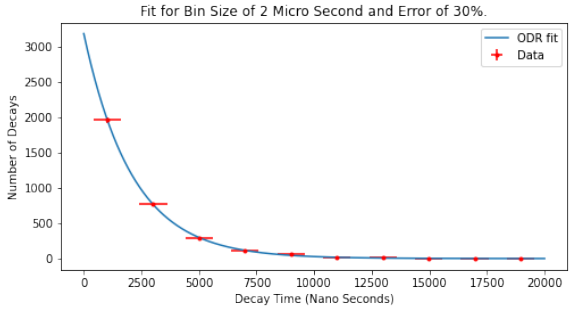

FIG. 6.

Table 1. THE MEASURED CHARGE RATIO OF MUONS

Median momentum (GeV./c.)	Charge ratio	Statistical error (S.D.)
6·7	1·229	0·049
10·4	1·223	0·038
17·5	1·233	0·037
35	1·268	0·051
77	1·37	0·16
120	1·45	0·23
240 *	1·61	0·38
240 *	1·40	0·45

* The measurements made at this momentum have been made by two different methods and are not statistically independent.

FIG. 7. Charge Ratio of Muons Across Different Momentums[4]

V. CONCLUSION

In conclusion, the effective measurement of the mean decay time at rest for a muon was made along with the derivation of the Fermi coupling constant and the charge ratio of positive to negative muons. The result with the best fit indicates that the mean lifetime decay for muons at rest is $t_{decay} = 2.10\mu s \pm 0.06\mu s$ which agrees closely with literature values. The derivation of the Fermi coupling constant indicates that the constant $G_F = 1.20 \times 10^{-5} \pm 0.06 \times 10^{-5}(GeV)^{-2}$ which also agrees with literature values and proves that muons undergo beta decay which is governed by the weak force. Finally, the Charge ratio at ground level was $\rho = 1.55 \pm 0.02$ proving that negatively charged muons occupy an orbital otherwise occupied by an electron.

[1] P. D. Group, P. A. Zyla, R. M. Barnett, J. Beringer, O. Dahl, D. A. Dwyer, D. E. Groom, C. J. Lin, K. S. Lugovsky, E. Pianori, D. J. Robinson, C. G. Wohl, W. M. Yao, K. Agashe, G. Aielli, B. C. Allanach, C. Amsler, M. Antonelli, E. C. Aschenauer, D. M. Asner, H. Baer, S. Banerjee, L. Baudis, C. W. Bauer, J. J. Beatty, V. I. Belousov, S. Bethke, A. Bettini, O. Biebel, K. M. Black, E. Blucher, O. Buchmuller, V. Burkert, M. A. Bychkov, R. N. Cahn, M. Carena, A. Ceccucci, A. Cerri, D. Chakraborty, R. S. Chivukula, G. Cowan, G. D'Ambrosio, T. Damour, D. de Florian, A. de Gouvêa, T. DeGrand, P. de Jong, G. Dissertori, B. A. Dobrescu, M. D'Onofrio, M. Doser, M. Drees, H. K. Dreiner, P. Eerola, U. Egede, S. Eidelman, J. Ellis, J. Erler, V. V. Ezhela, W. Fetscher, B. D. Fields, B. Foster, A. Freitas, H. Gallagher, L. Garren, H. J. Gerber, G. Gerbier, T. Gershon, Y. Gershtein, T. Gherghetta, A. A. Godizov, M. C. Gonzalez-Garcia, M. Goodman, C. Grab, A. V. Gritsan, C. Grojean, M. Grünewald, A. Gurtu, T. Gutsche, H. E. Haber, C. Hanhart, S. Hashimoto, Y. Hayato, A. Hebecker, S. Heinemeyer, B. Heltsley, J. J. Hernández-Rey, K. Hikasa, J. Hisano, A. Höcker, J. Holder, A. Holtkamp, J. Huston, T. Hyodo, K. F. Johnson, M. Kado, M. Karliner, U. F. Katz, M. Kenzie, V. A. Khoze, S. R. Klein, E. Klempt, R. V. Kowalewski, F. Krauss, M. Kreps, B. Krusche, Y. Kwon, O. Lahav, J. Laiho, L. P. Lellouch, J. Lesgourgues, A. R. Liddle, Z. Ligeti, C. Lippmann, T. M. Liss, L. Littenberg, C. Lourengo, S. B. Lugovsky, A. Lusiani, Y. Makida, F. Maltoni, T. Mannel, A. V. Manohar, W. J. Marciano, A. Masoni, J. Matthews, U. G. Meißner, M. Mikhasenko, D. J. Miller, D. Milstead, R. E. Mitchell, K. Mönig, P. Molaro, F. Moortgat, M. Moskovic, K. Nakamura, M. Narain, P. Nason, S. Navas, M. Neubert, P. Nevski, Y. Nir, K. A. Olive, C. Patrignani, J. A. Peacock, S. T. Petcov, V. A. Petrov, A. Pich, A. Piepke, A. Pomarol, S. Profumo, A. Quadt, K. Rabbertz, J. Rademacker, G. Raffelt, H. Ramani, M. Ramsey-Musolf, B. N. Ratcliff, P. Richardson, A. Ringwald, S. Roesler, S. Rolli, A. Romaniouk, L. J. Rosenberg, J. L. Rosner, G. Rybka, M. Ryskin, R. A. Ryutin, Y. Sakai, G. P. Salam, S. Sarkar, F. Sauli, O. Schneider, K. Scholberg, A. J. Schwartz, J. Schwiening, D. Scott, V. Sharma, S. R. Sharpe, T. Shutt, M. Silari, T. Sjöstrand, P. Skands, T. Skwarnicki, G. F. Smoot, A. Soffer, M. S. Sozzi, S. Spanier, C. Spiering, A. Stahl, S. L. Stone, Y. Sumino, T. Sumiyoshi, M. J. Syphers, F. Takahashi, M. Tanabashi, J. Tanaka, M. Taševský, K. Terashi, J. Terning, U. Thoma, R. S. Thorne, L. Tiator, M. Titov, N. P. Tkachenko, D. R. Tovey, K. Trabelsi, P. Urquijo, G. Valencia, R. Van de Water, N. Varelas, G. Venanzoni, L. Verde, M. G. Vincter, P. Vogel, W. Vogelsang, A. Vogt, V. Vorobyev, S. P. Wakely, W. Walkowiak, C. W. Walter, D. Wands, M. O. Wascko, D. H. Weinberg, E. J. Weinberg, M. White, L. R. Wiencke, S. Willocq, C. L. Woody, R. L. Workman, M. Yokoyama, R. Yoshida, G. Zanderighi, G. P. Zeller, O. V. Zenin, R. Y. Zhu, S. L. Zhu, F. Zimmermann, J. Anderson, T. Basaglia, V. S. Lugovsky, P. Schaffner, and W. Zheng, "Review of Particle Physics," *Progress of Theoretical and Experimental Physics*, vol. 2020, no. 8, 08 2020, 083C01. [Online]. Available: https://doi.org/10.1093/ptep/ptaa104

[2] B. Brau, C. May, R. Ormond, and J. Essick, "Determining the muon mass in an instructional laboratory," *American Journal of Physics*, vol. 78, no. 1, p. 64–70, 2010.

[3] R. L. Workman and Others, "Review of Particle Physics," *PTEP*, vol. 2022, p. 083C01, 2022.

[4] P. J. Hayman and A. W. Wolfendale, "Charge ratio of high-energy cosmic ray muons," vol. 195, no. 4837, pp. 166–167. [Online]. Available: https://www.nature.com/articles/195166a0